AEM
Journals.ASM.org

Molecular Analysis of the *Acinetobacter baumannii* Biofilm-Associated Protein

H. M. Sharon Goh,[a]* Scott A. Beatson,[a] Makrina Totsika,[a] Danilo G. Moriel,[a] Minh-Duy Phan,[a] Jan Szubert,[a] Naomi Runnegar,[b] Hanna E. Sidjabat,[c] David L. Paterson,[b,c,d] Graeme R. Nimmo,[b,c] Jeffrey Lipman,[d,e] Mark A. Schembri[a]

Australian Infectious Diseases Research Centre, School of Chemistry and Molecular Biosciences, The University of Queensland, Brisbane, Queensland, Australia[a]; Pathology Queensland Central Laboratory, Royal Brisbane and Women's Hospital, Brisbane, Queensland, Australia[b]; University of Queensland Centre for Clinical Research, Royal Brisbane and Women's Hospital, Brisbane, Queensland, Australia[c]; Royal Brisbane and Women's Hospital, Brisbane, Queensland, Australia[d]; Burns, Trauma and Critical Care Research Centre, University of Queensland, Brisbane, Queensland, Australia[e]

Acinetobacter baumannii* is a multidrug-resistant pathogen associated with hospital outbreaks of infection across the globe, particularly in the intensive care unit. The ability of *A. baumannii* to survive in the hospital environment for long periods is linked to antibiotic resistance and its capacity to form biofilms. Here we studied the prevalence, expression, and function of the *A. baumannii* biofilm-associated protein (Bap) in 24 carbapenem-resistant *A. baumannii* ST92 strains isolated from a single institution over a 10-year period. The *bap* gene was highly prevalent, with 22/24 strains being positive for *bap* by PCR. Partial sequencing of *bap* was performed on the index case strain MS1968 and revealed it to be a large and highly repetitive gene approximately 16 kb in size. Phylogenetic analysis employing a 1,948-amino-acid region corresponding to the C terminus of Bap showed that Bap_{MS1968} clusters with Bap sequences from clonal complex 2 (CC2) strains ACICU, TCDC-AB0715, and 1656-2 and is distinct from Bap in CC1 strains. By using overlapping PCR, the bap_{MS1968} gene was cloned, and its expression in a recombinant *Escherichia coli* strain resulted in increased biofilm formation. A Bap-specific antibody was generated, and Western blot analysis showed that the majority of *A. baumannii* strains expressed an ~200-kDa Bap protein. Further analysis of three Bap-positive *A. baumannii* strains demonstrated that Bap is expressed at the cell surface and is associated with biofilm formation. Finally, biofilm formation by these Bap-positive strains could be inhibited by affinity-purified Bap antibodies, demonstrating the direct contribution of Bap to biofilm growth by *A. baumannii* clinical isolates.

Acinetobacter baumannii is a Gram-negative bacterial pathogen associated with multidrug resistance and hospital outbreaks of infection, particularly in the intensive care unit (1). *A. baumannii* accounts for almost 80% of all reported *Acinetobacter* infections, including ventilator-associated pneumonia, bacteremia, meningitis, peritonitis, urinary tract infections, and wound infections (2, 3). The rapid emergence of multidrug-resistant *A. baumannii* strains has resulted in limited treatment options, with most strains being resistant to clinically useful antibiotics, such as aminoglycosides, fluoroquinolones, β-lactams (including carbapenems), tetracyclines, and trimethoprim-sulfamethoxazole (4, 5).

In addition to antibiotic resistance, the ability to form biofilms represents an important factor associated with *A. baumannii* virulence. Biofilms are sessile bacterial communities enclosed in a matrix comprised of extracellular material that can include polysaccharide, protein, and DNA (6). Biofilm formation by bacterial pathogens is associated with enhanced tolerance to host immune defenses, disinfectants, and antimicrobials (7, 8). *A. baumannii* strains readily form biofilms *in vitro*, and some of the molecular mechanisms associated with this phenotype have been studied; genes associated with biofilm formation include the *csu* locus (encoding the chaperone-usher Csu fimbriae), the *pga* locus (encoding the polysaccharide poly-*N*-acetylglucosamine [PNAG]), *ompA* (encoding the outer membrane protein OmpA), and *bap* (encoding the biofilm-associated protein [Bap]) (9–15).

A. baumannii Bap (Bap_{Ab}) is a cell surface protein associated with biofilm formation. In the *A. baumannii* bloodstream isolate 307-0294, $Bap_{Ab307\text{-}0294}$ is a large (854-kDa) protein comprised of multiple copies of repeat elements (13). Mutation of *bap* in *A. baumannii* 307-0294 resulted in decreased biofilm growth and decreased adherence to human bronchial epithelial and neonatal keratinocyte cells (13, 16). Bap homologues have also been identified and characterized in other bacteria, including members of other genera typically associated with hospital-acquired infection, such as *Staphylococcus* (17), *Enterococcus* (18, 19), and *Pseudomonas* (20, 21). *Staphylococcus aureus* Bap (Bap_{Sa}) has been well characterized and is an important virulence factor that contributes to initial attachment, intercellular adhesion, and biofilm maturation (17, 22). Bap proteins from other organisms contribute to different stages of biofilm formation and adhesion to eukaryotic host cells (17, 22).

We previously assessed the molecular epidemiology of *A. baumannii* within a single, large institution and showed that *A. baumannii* strains from sequence type 92 (ST92) were dominant over a 10-year period (5). In this study, we examined the role of Bap in these *A. baumannii* ST92 strains. We show that almost all *A. baumannii* ST92 strains express Bap and that its expression is strongly associated with biofilm formation. This is the first analysis of Bap

Received 30 April 2013 Accepted 7 August 2013
Published ahead of print 16 August 2013
Address correspondence to Mark A. Schembri, m.schembri@uq.edu.au.
* Present address: H. M. Sharon Goh, Singapore Centre on Environmental Life Sciences Engineering, School of Biological Sciences, Nanyang Technological University, Singapore.

doi:10.1128/AEM.01402-13

TABLE 1 Prevalence and expression of *bap* in *A. baumannii* ST92 clinical isolates

Isolate	*bap* gene[a]	Bap expression[b]	Yr of isolation	Previous designation[c]
MS1962	+	+	2004	Q11
MS1966	+	+	2001	Q5
MS1968	+	+	2001	Q6
MS1970	+	+	2001	Q7
MS1972	+	+	2000	
MS1976	−	+	2000	
MS1978	+	+	2000	
MS1980	+	+	2004	Q10
MS1984	+	+	2006	Q15
MS2992	+	+	2005	Q12
MS2993	+	+	2006	Q13
MS2995	+	+	2006	Q16
MS2996	+	+	2006	Q17
MS2998	+	+	2006	Q19
MS3000	+	+	2006	Q21
MS3002	+	+	2007	
MS3003	−	+	2007	
MS3004	+	+	2008	Q25
MS3005	+	+	2008	Q26
MS3007	+	−	2008	Q28
MS3009	+	+	2008	
MS3010	+	+	2008	
MS3011	+	+	2009	
MS3014	+	+	2009	

[a] Determined by PCR.
[b] Determined by Western blot analysis.
[c] Strain designation reported in reference 5.

function in *A. baumannii* ST92 strains associated with hospital infection outbreaks.

MATERIALS AND METHODS

Bacterial strains, plasmids, and growth conditions. Twenty-four carbapenem-resistant ST92 clinical isolates were selected from a collection of *A. baumannii* (isolated between 1999 and 2009) that caused sporadic and outbreak cases at the Royal Brisbane and Women's Hospital, Brisbane, Australia (Table 1), some of which have been described previously (5). The *Escherichia coli* strains MS2989 (DH10β containing plasmid pSG25; bap_{MS1968} in pBR322) and MS3640 (DH10β containing the vector control plasmid pBR322) were used. *A. baumannii* strains were routinely grown at 28°C in tryptic soy broth (TSB; Becton, Dickinson) supplemented with ampicillin (100 μg/ml) or kanamycin (50 μg/ml) as required. *E. coli* strains were cultivated in Luria-Bertani (LB) medium supplemented with ampicillin (100 μg/ml) as required.

DNA manipulations and genetic techniques. Chromosomal DNA was extracted from *A. baumannii* strains by previously described methods (23). PCR was performed using either *Taq* polymerase (New England BioLabs) or an Expand long-template PCR system (Roche) according to the manufacturer's instructions. PCR products were purified using a QIAquick PCR purification kit or a QIAquick gel extraction kit with spin columns according to the manufacturer's instructions (Qiagen). Standard cloning techniques were employed to construct recombinant plasmids (24); plasmid DNA was isolated using a QIAprep spin miniprep or midiprep kit (Qiagen). DNA sequencing reactions were carried out with an ABI BigDye terminator sequencing kit (version 3.1) (Applied Biosystems).

PCR screening of the *bap* gene. The 24 ST92 *A. baumannii* clinical isolates were screened for the presence of the *bap* gene by using primers 1415F (5′-TACTTCCAATCCAATGCTAGGGAGGGTACCAATGCAG) and 1416R (5′-TTATCCACTTCCAATGATCAGCAACCAAACCGCTAC). This gene region corresponded to the region selected for anti-Bap serum production.

Size determination and cloning of the *bap* gene. In order to ascertain the exact size of the MS1968 *bap* gene, a long-range PCR was performed using Expand long-template PCR system 1 (primers 1649F [5′-CTAGCCAACCATGCATGATCCAAAT] and 1652R [5′-GCGCGGGATCCGCATGAACTCTTTCAAAGCTAGG]). Amplification products were then resolved on a low-percentage-agarose gel using the lambda DNA/HindIII marker (Fermentas) as a reference, and the product size was estimated using Bio-Rad Image Lab software (Bio-Rad). For cloning *bap* into pBR322, the *bap* gene of MS1968 was amplified in two sections: the 5′ fragment (primers 1649F and 1650R [GCGCGGGATCCTTTAAAGGTTGCGGTTCCAG]) and the 3′ fragment (1651F [5′-CTTGGTAGGCGGAGCAGTAG] and 1652R. The 5′ fragment was digested with BmtI/BamHI and ligated into the *Bmt*I/BamHI sites of pBR322 to generate plasmid pSG24. Screening primers 1415F and 1416R were used to verify the presence of the 5′ *bap* fragment on pSG24, and primers 831F (5′-GCGCTCATCGTCATCCTC) and 1161R (5′-CCCTTATGCGACTCCTGC), which target the plasmid at the junction sites, were used to verify the cojoining plasmid-insert region by sequencing. The 3′ fragment was digested with BsrGI/BamHI and ligated into the BsrGI/BamHI sites of pSG24 to generate pSG25. This plasmid was verified by sequencing the 5′ and 3′ joining sites. The confirmed clone (MS2989) was then tested for Bap expression and biofilm formation.

DNA sequencing, assembly and bioinformatics. The sequence of the bap_{MS1968} gene in pSG25 was determined by primer walking and Sanger sequencing, and sequence reads were manually assembled using Vector NTI Advance software (Life Technologies). The assembled DNA sequence of bap_{MS1968} was compared against $bap_{AB307\text{-}0294}$ using Easyfig (25). The C-terminal sequence of Bap_{MS1968} (1,948 amino acids) was determined using the BLASTp program (NCBI) and aligned with Bap homologues obtained from the NCBI database using Vector NTI Advance and ClustalW2 (26). The alignment generated using Vector NTI Advance was used to determine the region within Bap homologues that corresponded with the C-terminal sequence of Bap_{MS1968}. A neighbor-joining tree was generated using MEGA5 (27) by comparing 1,948 amino acids from the C-terminal sequence of Bap_{MS1968} against amino acid sequences of Bap homologues identified in the NCBI database.

Generation of Bap polyclonal antiserum, affinity purification, and immunoblotting. A polyclonal antibody against Bap_{MS1968} was prepared by amplifying a 1,254-bp segment of the bap_{MS1968} gene using primers 1415F and 1416R with ligation-independent cloning (LIC) overhangs flanking both ends of the primers to enable cloning into the pMCSG7 6-histidine N-terminally tagged expression vector (28). The resultant plasmid (pSG13) contained base pairs 132 to 1,386 of bap_{MS1968} fused to an N-terminal 6×His-encoding sequence. This *bap* sequence corresponds to amino acid residues 45 to 462 (418 amino acids) of the Bap_{MS1968} sequence. *E. coli* BL21 was transformed with plasmid pSG13, and the desired clones were confirmed by PCR and sequencing using primers 1508F (5′-TAATACGACTCACTATAGGG) and 1509R (5′-TATGCTAGTTATTGCTCAG). MS2788 (BL21+pSG13) was induced with 1 mM isopropyl β-D-1-thiogalactopyranoside (IPTG), and the resultant fusion protein was purified using a Qiagen nickel-nitrilotriacetic acid (Ni-NTA) spin kit according to the manufacturer's instructions. Protein was assessed for purity by SDS-PAGE analysis and quantified using a bicinchoninic acid kit (Sigma-Aldrich) (29). A polyclonal anti-Bap serum was raised in rabbits at the Institute of Medical and Veterinary Sciences (Adelaide, South Australia, Australia).

Affinity chromatography was used to purify Bap-specific antibodies from the rabbit polyclonal anti-Bap serum as follows. A 30-ml culture of MS2788 was grown at 37°C to an optical density at 600 nm (OD_{600}) of 0.6 in the presence of 1 mM IPTG. Cells were pelleted via centrifugation and resuspended in chilled sonication buffer (25 mM Tris, 150 mM NaCl [pH 7.0]). The suspension was sonicated three times with a 30-s burst and a 2-min incubation on ice between bursts. The cell extract was centrifuged

at 12,000 × *g* for 20 min at 4°C. The column was prepared using a 1-ml bed volume of Talon cobalt metal affinity resin (Clontech) and equilibrated using 5 ml of equilibration/wash buffer (25 mM Tris, 10 mM NaCl [pH 7.0]). The MS2788 cell lysate was applied to the column, and nonspecific proteins were removed using 20 ml of equilibration/wash buffer. An aliquot of the polyclonal Bap antiserum was diluted with an equal volume of Tris-buffered saline (TBS) buffer (pH 7.2 to 7.4) and applied to the affinity column. Nonspecific proteins were removed using equilibration/wash buffer. Bap-specific antibodies bound on the column were eluted using a gentle antigen-antibody (Ag/Ab) elution buffer, pH 6.6 (Pierce). A 30-kDa desalting column (Millipore) was used to concentrate and exchange the purified antibodies into TBS buffer. Flowthrough fractions were collected at every step of purification for SDS-PAGE and immunoblotting analysis. Immunoblotting was performed as previously described (29). A 1:200 dilution of affinity-purified Bap-specific antibodies was used as primary serum, and the secondary antibody was alkaline phosphatase-conjugated anti-rabbit IgG (Sigma-Aldrich).

Extracellular matrix (ECM) protein binding assays. ECM protein binding by *A. baumannii* to MaxGel human ECM (Sigma-Aldrich) was performed as described previously, with the exception that wells were washed with phosphate-buffered saline (PBS) and quenched with 2% bovine serum albumin (BSA) in PBS for 1 h, and overnight bacterial cultures were standardized to an OD_{600} of 1.0 (30). For negative-control wells, PBS was added instead of bacteria. Instead of an enzyme-linked immunosorbent assay (ELISA), adherent cells were stained with 0.01% crystal violet for 30 min at room temperature. Wells were washed twice with PBS and incubated with 200 μl ethanol/acetone (80:20) for 1 h at room temperature with gentle agitation. Absorbance measurements were obtained at 595 nm, and results were analyzed by analysis of variance (ANOVA) (GraphPad Prism 5 software).

Biofilm study. Biofilm formation by *A. baumannii* on 96-well polystyrene plates (Iwaki) was performed by previously described protocols, except that strains were grown at 28°C in TSB under static conditions (31). Biofilm formation by DH10β was performed as described above, except that cells were grown with shaking in polyvinylchloride (PVC) microtiter plates containing M9 supplemented with 0.3% Casamino Acids. Briefly, strains were grown as shaking cultures at 250 rpm for 20 h at 28°C in the appropriate culture medium supplemented with antibiotics, inoculated into microtiter plates with fresh medium, and incubated for 24 h at 28°C; wells were washed to remove unbound cells and subsequently stained with 0.01% crystal violet. Bound cells were quantified by addition of ethanol-acetone (80:20) and measurement of the solubilized stain at an optical density of 595 nm using a Spectramax 250 microtiter plate reader with SOFTmax Pro v2.2.1 software (Molecular Devices). Readings obtained were analyzed by ANOVA (GraphPad Prism 5 software). These experiments were performed in eight replicates. Inhibition of biofilm formation using Bap affinity-purified antibody was performed using the microtiter plate biofilm protocol mentioned for *A. baumannii*, except that Bap-specific antibodies were added to a final concentration of 1:10 before addition of bacteria to the polystyrene plate. Readings obtained were analyzed by ANOVA. This experiment was performed in quadruplicate. Flow chamber biofilm experiments were performed as previously described (32), except that cells were grown in TSB supplemented with ampicillin and detected using 0.1 μM BacLight green fluorescent stain (Molecular Probes). Briefly, biofilms were allowed to form on glass surfaces in a multichannel flow system that permitted online monitoring of community structures. Flow cells were inoculated with standardized overnight cultures grown in TSB. Biofilm development was monitored by confocal laser scanning microscopy (CLSM) from 19 to 48 h postinoculation. This experiment was performed in duplicate.

Microscopy and image analysis. An anti-Bap serum was used for immunofluorescence microscopy as previously described (33), with modifications where strains were grown in TSB and a 1:5 dilution of the primary antibody was used followed by goat anti-rabbit IgG antibody conjugated to fluorescein isothiocyanate (FITC) (1:500) as the secondary antibody. Microscopic observation of biofilms and image acquisition was performed on a confocal laser scanning microscope (LSM510 Meta; Zeiss). Vertical cross sections through the biofilms were visualized using the Zeiss LSM image examiner, and the *z* stacks were analyzed using COMSTAT software (34). Results were analyzed by ANOVA (Minitab Statistical Software). Images were further processed for display by using Photoshop software (Adobe Systems).

Protein sequence accession number. The sequence of Bap_{MS1968} has been submitted to the GenBank database under accession numbers AGM37925.

RESULTS

The *bap* gene is highly prevalent in *A. baumannii* ST92 strains. Twenty-four carbapenem-resistant *A. baumannii* ST92 strains isolated from a single institution during a 10-year period from 1999 to 2009 were examined for the presence of the *bap* gene. Initially, a draft genome sequence of one strain, MS1968, was determined, and this provided a partial sequence for *bap*, albeit with gaps in the large repeat regions. Based on this sequence, primers 1415F and 1416R were designed to amplify a 1,225-bp segment of bap_{MS1968} from a nonrepetitive region. PCR analysis was performed on all 24 *A. baumannii* ST92 strains, and a product of the correct size was detected in 91.7% (22/24) of the strains, demonstrating that the *bap* gene is highly prevalent in our collection (Table 1).

Cloning of the *bap* gene from *A. baumannii* MS1968. Based on the draft genome sequence of *A. baumannii* MS1968 and preliminary PCR assays, the size of bap_{MS1968} was estimated to be approximately 16 kb (data not shown). In order to clone bap_{MS1968}, two overlapping PCR amplicons were generated (a 12,144-bp fragment containing the 5′ region and a 4,170-bp fragment containing the 3′ region). These fragments were cloned into plasmid pBR322 in a two-step process to generate plasmid pSG25, which contained the full-length bap_{MS1968} gene.

Sequencing of bap_{MS1968} and comparative analysis with other *bap* genes. In order to close the gap within the bap_{MS1968} gene from the draft genome sequence, the sequence of bap_{MS1968} was determined from plasmid pSG25 using a primer walking strategy. Approximately 9.5 kb of bap_{MS1968}, including 3,783 bp of the 5′ region and 5,847 bp of the 3′ region, was sequenced, leaving an estimated 5,500-bp gap that could not be closed by this method (Fig. 1). A nucleotide sequence alignment using ClustalW2 indicated that bap_{MS1968} and $bap_{AB307\text{-}0294}$ share approximately 50% sequence identity (Fig. 1). The ~5,500-bp unsequenced region of bap_{MS1968} is most likely made up of the core repeat module D, thus causing the eventual sequencing problems.

Analysis of the 5,847-bp segment corresponding to the 3′ region of bap_{MS1968} revealed an in-frame translated sequence comprising 1,948 amino acids. An amino acid sequence alignment using ClustalW2 indicated that this region of Bap_{MS1968} shares 37% sequence identity with the corresponding region of $Bap_{AB307\text{-}0294}$ (residues 6,669 to 8,620). The amino acid sequence similarity of Bap_{MS1968} with other Bap proteins was evaluated using MEGA5 (27). Figure 2 illustrates a neighbor-joining tree constructed using aligned Bap amino acid sequences from 26 bacterial strains. A consensus tree of 1,000 bootstrap replicates revealed two major clades. The two clades separate the majority of the Gram-negative and Gram-positive Bap proteins (with the exception of *Bordetella bronchiseptica*, *Pseudomonas fluorescens*, and *Pseudomonas putida*). The predicted Bap protein homologues of *A. baumannii* cluster within the large clade of the Gram-negative Bap homologues. A scheme for classi-

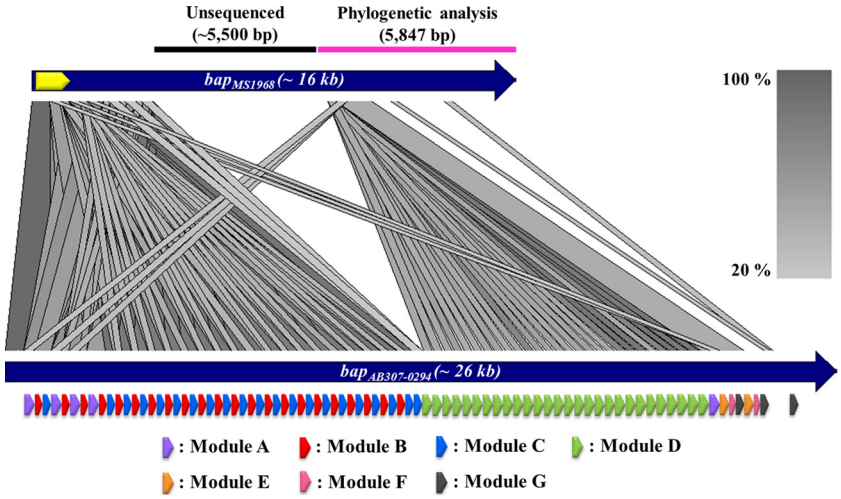

FIG 1 Physical representation of the nucleotide sequence alignment between bap_{MS1968} (GenBank accession no. KC981110) and $bap_{AB307\text{-}0294}$ (EU117203) (13). The size of bap_{MS1968} was determined by PCR (~16 kb), and the sequence was obtained by primer walking. The black bar indicates the region (5,500 bp) that could not be sequenced using primer walking. The yellow arrow indicates the region (1,254 bp) cloned and expressed for antibody production. The magenta bar indicates the region (5,847 bp) selected for phylogenetic analysis (Fig. 3). This figure was generated using Easyfig (http://easyfig.sourceforge.net/) with nucleotide sequence comparison (BLASTn) (25). The level of nucleotide identity is shown in the gradient scale.

fying *A. baumannii* into clonal complexes (CC) was proposed by Diancourt et al. in 2010 and reported AB307-0294, AB0057, and AYE as representatives of CC1, whereas European clone II isolates ACICU, TCDC-AB0715, and 1656-2 represented CC2 (35–37). Consistent with this scheme, Bap_{MS1968} clustered together with Bap from other CC2 strains. The separate clustering of CC1 and CC2 Bap proteins indicates the presence of Bap variants within *A. baumannii*.

We also examined the genetic context of *bap* in *A. baumannii*. Based on the draft genome sequence of MS1968, the chromosomal location of bap_{1968} is identical to that previously described for *A. baumannii* 307-0294 (38). The *bap* gene appears to be disrupted in many complete *A. baumannii* genome sequences available in public databases, a consequence of its intrinsic repetitive features that might be an obstacle for the correct assembly of its coding region. We selected the complete genome sequences of *Acinetobacter* species in which *bap* appeared to be correctly assembled and compared the corresponding genomic regions (Fig. 3A). Bap from AB307-0294 is 94.7% identical at the amino acid level to Bap from AYE and BJAB0715; however, this is reduced significantly compared to Bap from PHEA-2 (67.9% amino acid identity), Bap from ADP1 (28.5% amino acid identity), and Bap from SDF (27.6% amino acid identity). Despite these differences, *bap* is located at the same genome position in all six strains, flanked by a core and a variable region. The core upstream region is represented by genes encoding succinyl coenzyme synthetase (*sucCD*), a tricarboxylic cycle enzyme that catalyzes the interconversion of succinyl coenzyme A (succinyl-CoA) and succinate, accompanied by the production or hydrolysis of GTP (39). The core downstream region contains genes encoding carbamoylphosphate synthetase (*carAB*), an intermediate in the biosynthesis of arginine and pyrimidines (40), and *greA*, a transcriptional elongation factor with chaperone activity that inhibits aggregation of proteins under heat shock conditions and promotes the refolding of denatured proteins (41). The variable flanking region of *bap* was not conserved in the *Acinetobacter* genomes analyzed and contained genes encoding hypothetical proteins, a gene encoding a putative Na^+/H^+ antiporter (ABBFA_000774), and genes encoding putative metalloproteases (ABBFA_000773 and ABBFA_000781). Finally, analysis of the intergenic regions up- and downstream of *bap* revealed the presence of palindromic repeats (Fig. 3B), suggesting that the variable regions may have been acquired through independent recombination events.

Expression of Bap by *E. coli* harboring pSG25 results in increased biofilm formation. To demonstrate functional expression of Bap from plasmid pSG25 in *E. coli*, a polyclonal antibody was generated against a conserved, nonrepetitive region within Bap_{MS1968}. SDS-PAGE and Western blot analysis of whole-cell lysates of MS2989 (*E. coli* DH10β containing pSG25) grown in LB broth identified an ~200-kDa protein that reacted with the Bap-specific antiserum (data not shown). A microtiter plate biofilm assay demonstrated that expression of the *bap* gene by DH10β resulted in significantly increased biofilm formation by MS2989 compared to the vector control strain (MS3640) (Fig. 4). Thus, Bap can be expressed by *E. coli*, and its expression leads to increased biofilm formation.

Bap is expressed by most *A. baumannii* ST92 isolates. To investigate the expression of Bap in our collection of 24 *A. baumannii* ST92 strains, whole-cell lysates were prepared from each strain following overnight shaking growth in TSB and examined by Western blot analysis using the Bap-specific antibody described above. A strong Bap-specific cross-reacting band was detected at ~200 kDa in all but one of the 24 strains tested (95.8%; Table 1). This analysis identified inconsistencies with respect to the PCR prevalence assay; strains MS1976 and MS3003 expressed Bap but were negative in the PCR screen for the *bap* gene, while MS3007 failed to express Bap but was positive in the PCR screen. Out of the 24 ST92 strains, four strains were selected for further analysis of Bap expression and function, three strains positive for Bap expression (MS3009, MS3011 and MS3014) and one strain negative for Bap expression (MS3007) (Fig. 5A).

Bap is located at the cell surface. The cellular localization of

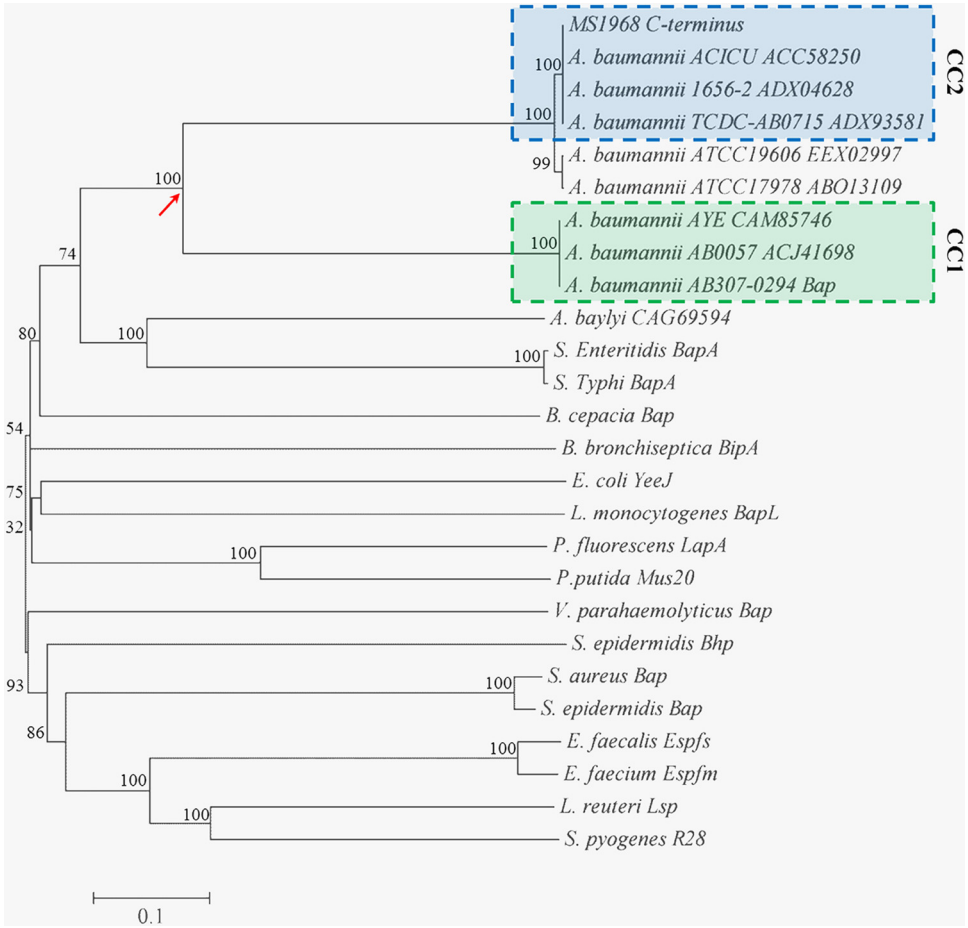

FIG 2 Neighbor-joining tree indicating sequence similarity of Bap_{MS1968} (GenBank accession no. AGM37925) in relation to Bap homologues from *A. baumannii* strains (TCDC-AB0715 [accession number ADX93581]; ACICU [ACC58250, ACC58252 to ACC58258]; 1656-2 [ADX04628 to ADX04634]; ATCC 19606 [EEX02997]; ATCC 17978 [ABO13109]; AB307-0294 [ABX00640]; AYE [CAM85746]; AB0057 [ACJ41698]), *Acinetobacter baylyi* (CAG69594), *Burkholderia cepacia* (AAT36485), *Salmonella enterica* serovar Enteritidis (ABX46037), *Salmonella enterica* serovar Typhi (NP_806354), *Vibrio parahaemolyticus* (NP_800463), *Escherichia coli* (ACB16711), *Listeria monocytogenes* (CAC98514), *Staphylococcus aureus* (AAK38834), *Staphylococcus epidermidis* (AAY28519 and AAK29746 [Bhp]), *Bordetella bronchiseptica* (AAG53941), *Pseudomonas fluorescens* (AAY95545), *Pseudomonas putida* (NP_742337), *Enterococcus faecalis* (AAD09858), *Enterococcus faecium* (EFF33494), *Lactobacillus reuteri* (EDX43426), and *Streptococcus pyogenes* (AAD39085). Sequences were aligned using ClustalW2, and the phylogenetic tree was generated in MEGA5 by comparing 1,948 amino acids from the C-terminal sequence of Bap_{MS1968}. Numbers at the branches indicate confidence values determined from 1,000 bootstrap replications. The *A. baumannii* Bap proteins cluster according to their CC designations; a CC has not been proposed for the ATCC strains. The red arrow indicates the most recent common ancestor shared by CC1 and CC2 Bap proteins. The two major clades demonstrate separate clustering of Gram-negative and Gram-positive Bap homologues (with the exception of *L. monocytogenes* and *V. parahaemolyticus*).

Bap in *A. baumannii* ST92 strains was investigated by immunofluorescence microscopy employing our affinity-purified Bap antibody. Consistent with the Western blot analysis (Fig. 5A), the Bap antiserum reacted with MS3009, MS3011, and MS3014. In contrast, no reaction was observed for MS3007 (Fig. 5B). Thus, Bap is effectively expressed and is localized on the cell surfaces of *A. baumannii* strains MS3009, MS3011, and MS3014.

Bap_{Ab} does not mediate binding to ECM molecules. The four strains selected for Bap characterization (MS3007, MS3009, MS3011, and MS3014) were tested for their ability to bind MaxGel, a commercially available mixture of human ECM components, including collagens, laminin, fibronectin, tenascin, elastin, and a number of proteoglycans and glycosaminoglycans. None of the strains displayed significant binding to MaxGel in this assay (data not shown), suggesting that Bap expression by MS3009, MS3011, and MS3014 does not lead to adherence to ECM components under the conditions used in this experiment.

Expression of Bap is associated with strong biofilm formation. Biofilm formation by *A. baumannii* was examined using dynamic and static biofilm assays. The continuous flow chamber method was used to test the ability of Bap to promote biofilm formation under dynamic conditions, which permits monitoring of the bacterial distribution within an evolving biofilm at the single-cell level using scanning confocal laser microscopy. In this assay, the Bap-positive strains MS3009, MS3011, and MS3014 formed a dense, mat-like biofilm across the glass surface with significantly higher substratum coverage (53.26%, 60.7%, and 60.38%, respectively) than the Bap-negative strain MS3007 (29.96%; $P = 0.002$) (Fig. 6). In the static microtiter plate assay, the Bap-positive strains MS3009, MS3011, and MS3014 produced a strong biofilm compared to the Bap-negative strain MS3007 ($P < 0.0001$) (Fig. 7). Taken together, these results demonstrate that the Bap-expressing *A. baumannii* strains MS3009, MS3011, and MS3014 can form strong bio-

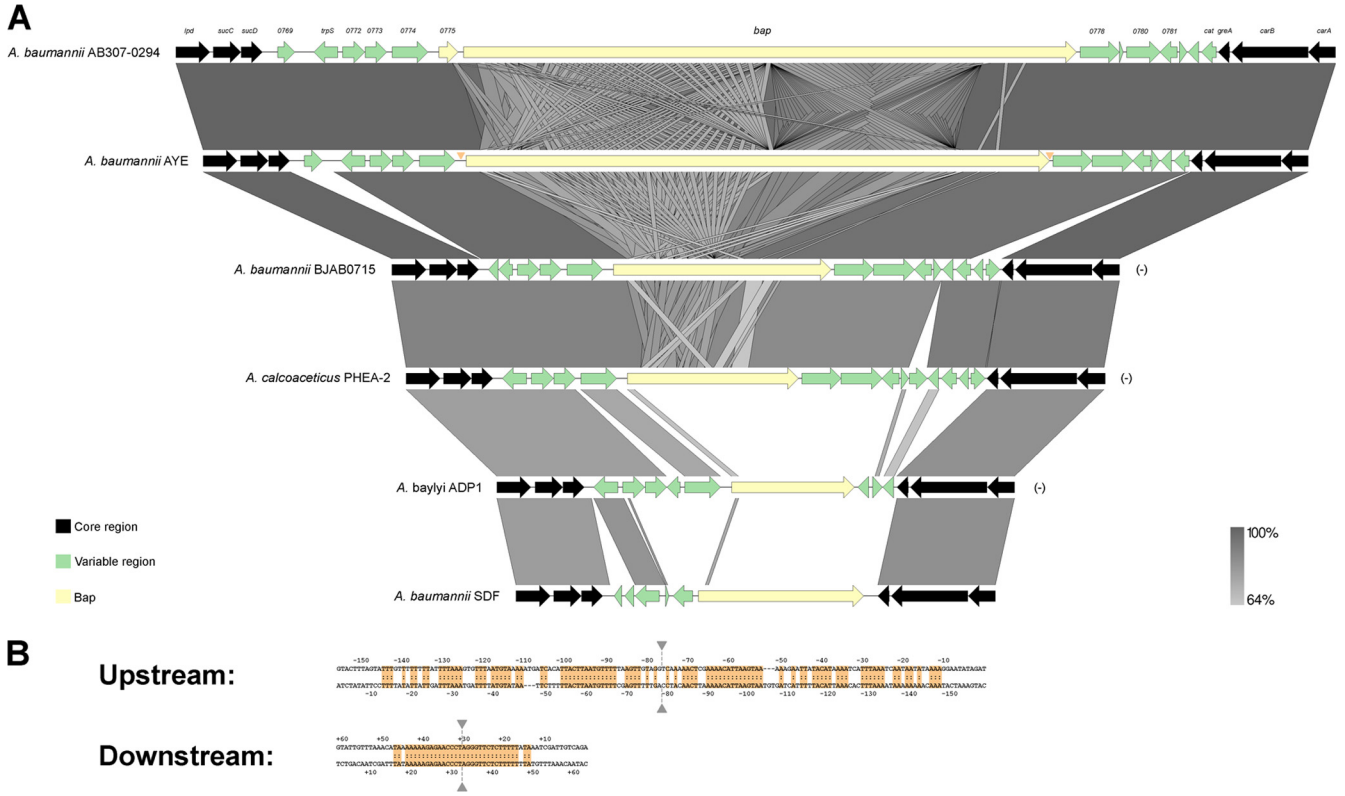

FIG 3 Genome context of the *bap* gene in *Acinetobacter*. (A) Genomic analysis of different *Acinetobacter* species indicates that *bap* is located at the same chromosomal position in all strains examined. The genome orientation was reversed for some strains to facilitate visualization (−). Also indicated are the respective core (black) and variable (green) regions flanking the *bap* gene. Orange triangles indicate the locations of sequence repeats. Genome alignments were performed using Easyfig (25). (B) Alignment of palindromic repeats localized upstream and downstream of the *bap* gene in *Acinetobacter*. The axis is indicated by a gray arrow.

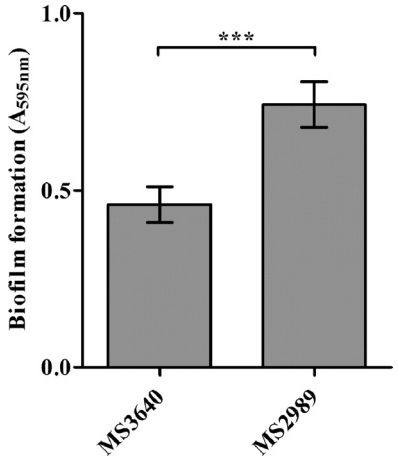

FIG 4 Microtiter plate biofilm formation by MS2989 in comparison to MS3640. Strains were grown under shaking conditions at 28°C for 24 h in polyvinyl chloride (PVC) microtiter plates containing M9 supplemented with 0.3% Casamino Acids. Plates were washed to remove nonadherent cells and stained with 0.01% crystal violet. Biofilm formation was quantified by solubilizing the crystal violet stain retained by adherent cells with ethanol-acetone (80:20) and measuring the absorbance at 595 nm. Results are the means for eight replicates per strain (± standard deviation). Mean values for MS3640 (0.4604) and MS2989 (0.7425) were calculated using GraphPad Prism 5 software ($P < 0.001$).

films, while MS3007, which does not express Bap, does not form a significant biofilm.

Bap is required for biofilm formation *in vitro*. To further characterize the role of Bap in biofilm formation by *A. baumannii* MS3009, MS3011, and MS3014, we performed microtiter plate biofilm assays in the presence of affinity-purified Bap-specific antibody. In these assays, the addition of 1:10-diluted Bap antibody inhibited biofilm formation by all three strains ($P < 0.0001$) (Fig. 7). These results provide compelling evidence that Bap plays an important role in biofilm formation by *A. baumannii* ST92 strains associated with hospital infection outbreaks.

DISCUSSION

A. baumannii strains from ST92 and the associated CC92 (also known as European clone 2 or worldwide clone 2) represent the most sampled and widespread *A. baumannii* sequence type across the globe. Antibiotic susceptibility within ST92 is variable, suggesting a role for mechanisms other than antibiotic resistance in its successful dissemination. In this study, we examined the prevalence, sequence, and function of Bap from a collection of *A. baumannii* ST92 strains isolated from a single institution over a 10-year period.

Bap was first detected in *S. aureus* strains that cause bovine mastitis (42). Subsequently, more Bap homologues have been identified and characterized from a range of Gram-positive and Gram-negative bacteria, including *A. baumannii* (13, 17–22,

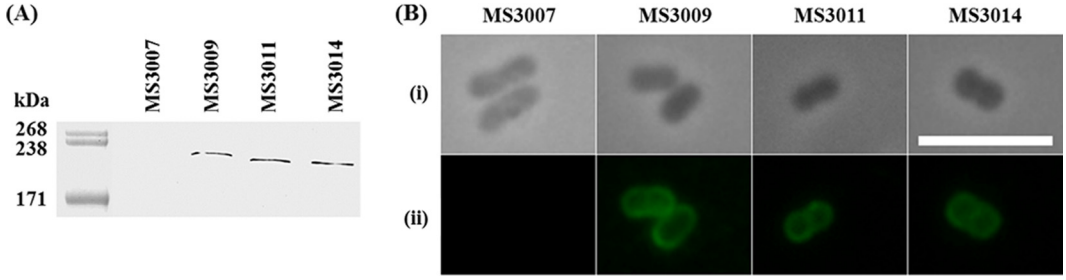

FIG 5 (A) Western blot obtained using Bap-specific antiserum showing expression of Bap (~200 kDa) in *A. baumannii* MS3009 (lane 3), MS3011 (lane 4), and MS3014 (lane 5) but not MS3007 (lane 2) from whole-cell lysates of overnight shaking cultures. Molecular mass markers (HiMark prestained protein standard) are indicated in lane 1. (B) Immunofluorescence microscopy demonstrating surface localization of Bap. Phase contrast (i) and fluorescence (ii) images of MS3007, MS3009, MS3011, and MS3014 cells following overnight growth with agitation at 28°C are shown. Bar, 5 μm.

43–51). Common features of Bap in all of these organisms include its large size, the presence of multiple tandem repeats, its cell surface location and its role in biofilm formation. In *Pseudomonas fluorescens*, a large-repeat Bap-like protein referred to as LapA contributes to surface attachment and biofilm formation (21). LapA is translocated to the cell surface by an ABC transporter encoded by the adjacent *lapEBC* genes (52). Similarly, in *Salmonella enterica* serovar Enteritidis, BapA is secreted by a type I protein secretion system (BapBCD) situated downstream of the *bapA* gene (46). Examination of the genetic location of *bap* in *A. baumannii* did not reveal any evidence of a system that could mediate its translocation. Thus, the mechanism by which Bap is transported to the surface of *A. baumannii* remains to be elucidated. We note that a small but significant increase in biofilm formation was observed in the recombinant *E. coli* MS2989 strain expressing Bap, indicating that there may be some level of redundancy in its mode of export. However, we were unable to definitively detect Bap expression on the surface of *E. coli* MS2989 by immunofluorescence microscopy, suggesting that the level of Bap was very low.

Our analysis revealed that the *bap* gene is highly prevalent in *A. baumannii* ST92 strains. All but one *A. baumannii* strain in our collection (i.e., MS3007) also expressed the Bap protein. The in-

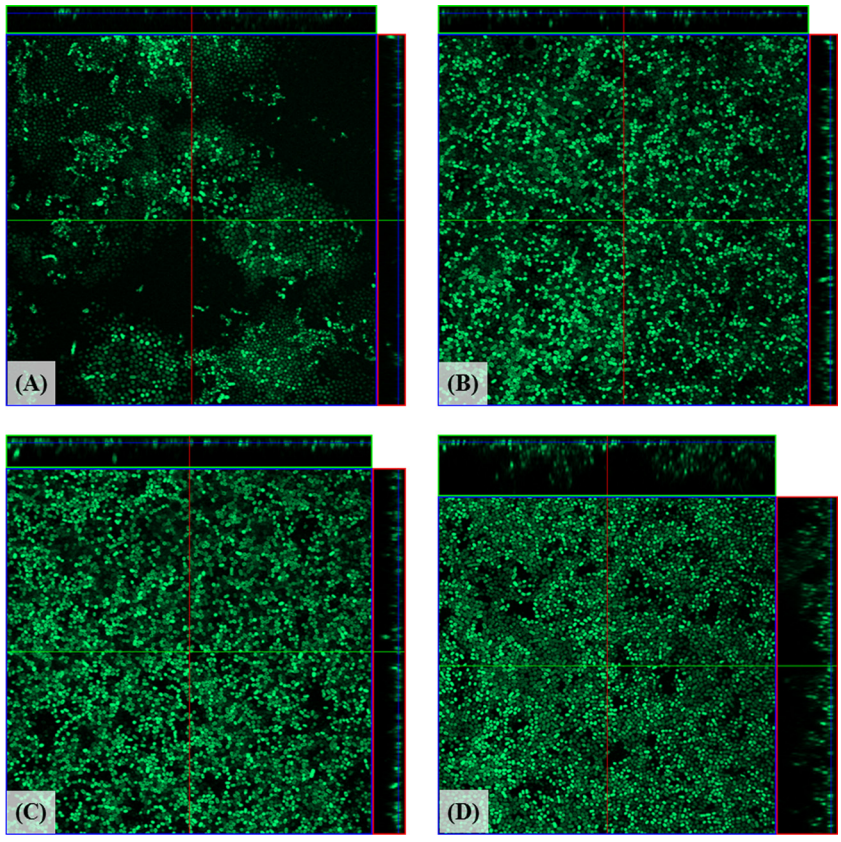

FIG 6 Flow chamber biofilm formation by MS3007 (A), MS3009 (B), MS3011 (C), and MS3014 (D). Biofilm development was monitored by CLSM 48 h postinoculation. Substratum coverage of each strain is as follows: MS3007, 29.96%; MS3009, 53.26%; MS3011, 60.7% and MS3014, 60.38% ($P = 0.002$). Micrographs represent horizontal sections. Depicted to the right of and below each panel are the *yz* plane and *xz* plane, respectively, at the positions indicated by the lines.

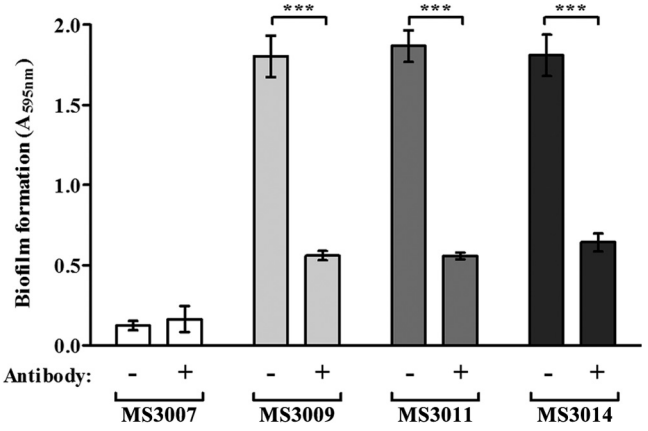

FIG 7 Microtiter plate assay demonstrating biofilm formation by MS3007, MS3009, MS3011, and MS3014. Biofilm inhibition was performed by supplementing respective wells with a 1:10 dilution of affinity-purified Bap antibodies in TSB to assess inhibitory effects on biofilm formation. Plates were incubated under static conditions at 28°C for 24 h then washed to remove nonadherent cells and subsequently stained with 0.01% crystal violet. Biofilm formation was quantified by solubilizing the crystal violet stain retained by adherent cells with ethanol-acetone (80:20) and measuring the absorbance at 595 nm. Results are the means of quadruplicates for each strain (± standard deviations).

consistencies between gene prevalence by PCR and protein expression are most likely due to sequence variation. It is possible that MS3007 harbors an incomplete or truncated *bap* gene. Indeed, Loehfelm et al. previously reported the presence of short homologous regions of $bap_{AB307\text{-}0294}$ within the genome sequence of *A. baylyi* and *A. baumannii* ATCC 17978 (13).

The previously characterized *A. baumannii* $Bap_{AB307\text{-}0294}$ is a high-molecular-mass (854-kDa) protein consisting of multiple repeat regions (13). In contrast, the *A. baumannii* ST92 strains examined in this study all expressed a Bap protein of approximately 200 kDa. A partial sequence of the *bap* gene was obtained from one strain, MS1968, which represented the index case isolate from a small outbreak in 2001. Given that the *A. baumannii* MS1968 *bap* gene is ~16 kb, we expected it to encode a significantly larger protein. It is possible that Bap_{1968} is degraded or even processed; however, this remains to be determined. The difference in the size of the *bap* genes from *A. baumannii* strains MS1968 (~16 kb) and AB307-0294 (25.863 kb), despite their similar genetic context, also demonstrates that there is significant variation in the *bap* genes from different *A. baumannii* strains. The *A. baumannii* Bap protein contains a modular structure (53), and the presence of large, identical repeat sequences within module D of bap_{MS1968} prevented us from generating a complete sequence of the gene. However, we did identify a nonrepetitive sequence that was used to examine the phylogeny of Bap from several species. In comparison to $Bap_{AB307\text{-}0294}$ (which clustered in CC1), Bap_{MS1968} clustered in CC2. The two Bap sequences exhibited significant variation and displayed only 37% amino acid identity over this region. Further analysis of Bap from other CC1 and CC2 strains was consistent with this clustering, and suggests that the nonrepetitive sequence of Bap can differentiate between CC1 and CC2 strains. When analyzed in the context of Bap sequences from different organisms, all of the *A. baumannii* Bap homologues clustered uniquely. It remains to be determined if this nonrepetitive region of Bap is representative of its phylogenic distribution in comparison to the entire protein sequence. However, given the size and highly repetitive nature of Bap, this approach avoided the comparative analysis of regions that might potentially contain multiple sequence errors.

Several lines of evidence suggest that Bap contributes to biofilm formation by *A. baumannii* ST92. First, Bap expression by three *A. baumannii* strains was associated with strong biofilm growth, while the *A. baumannii* ST92 strain MS3007, which did not express Bap, did not form a biofilm in microtiter plate- and flow cell-based assays. Additionally, affinity-purified Bap-specific antibodies blocked Bap-mediated biofilm formation by *A. baumannii* strains MS3009, MS3011, and MS3014. Taken together, our results demonstrate a role for Bap in biofilm formation that is consistent with previous literature examining other *A. baumannii* strains (13, 16). Our results should provide the basis for more detailed studies to examine the translocation and function of Bap in *A. baumannii*, including other common multidrug-resistant sequence types associated with hospital infection outbreaks.

ACKNOWLEDGMENTS

This work was supported by grants from the Australian National Health and Medical Research Council, The University of Queensland, the Royal Brisbane and Women's Hospital, and the Royal Brisbane and Women's Hospital Foundation. M.A.S. was supported by an Australian Research Council (ARC) Future Fellowship (FT100100662). M.T. was supported by an ARC Discovery Early Career Researcher Award (DE130101169).

REFERENCES

1. **Doidge M, Allworth AM, Woods M, Marshall P, Terry M, O'Brien K, Goh HMS, George N, Nimmo GR, Schembri MA, Lipman DJ, Paterson DL.** 2010. Control of an outbreak of carbapenem-resistant *Acinetobacter baumannii* in Australia after introduction of environmental cleaning with a commercial oxidising disinfectant. Infect. Control Hosp. Epidemiol. **31:**418–420.
2. **Bergogne-Berezin E, Towner KJ.** 1996. *Acinetobacter* spp. as nosocomial pathogens: microbiological, clinical, and epidemiological features. Clin. Microbiol. Rev. **9:**148–165.
3. **Centers for Disease Control and Prevention USA.** 2004. Drug-resistant *Acinetobacter* infections in healthcare settings, vol 2009. Department of Health and Human Services, Atlanta, GA.
4. **Peleg AY, Seifert H, Paterson DL.** 2008. *Acinetobacter baumannii*: emergence of a successful pathogen. Clin. Microbiol. Rev. **21:**538–582.
5. **Runnegar N, Sidjabat H, Goh HMS, Nimmo GR, Schembri MA, Paterson DL.** 2010. Molecular epidemiology of multidrug-resistant *Acinetobacter baumannii* in a single institution over a 10-year period. J. Clin. Microbiol. **48:**4051–4056.
6. **Hall-Stoodley L, Costerton JW, Stoodley P.** 2004. Bacterial biofilms: from the natural environment to infectious diseases. Nat. Rev. Microbiol. **2:**95–108.
7. **Fux CA, Costerton JW, Stewart PS, Stoodley P.** 2005. Survival strategies of infectious biofilms. Trends Microbiol. **13:**34–40.
8. **Sakuragi Y, Kolter R.** 2007. Quorum-sensing regulation of the biofilm matrix genes (*pel*) of *Pseudomonas aeruginosa*. J. Bacteriol. **189:**5383–5386.
9. **Choi AH, Slamti L, Avci FY, Pier GB, Maira-Litran T.** 2009. The *pgaABCD* locus of *Acinetobacter baumannii* encodes the production of poly-β-1-6-*N*-acetylglucosamine, which is critical for biofilm formation. J. Bacteriol. **191:**5953–5963.
10. **Dorsey CW, Tomaras AP, Connerly PL, Tolmasky ME, Crosa JH, Actis LA.** 2004. The siderophore-mediated iron acquisition systems of *Acinetobacter baumannii* ATCC 19606 and *Vibrio anguillarum* 775 are structurally and functionally related. Microbiology **150:**3657–3667.
11. **Gaddy JA, Actis LA.** 2009. Regulation of *Acinetobacter baumannii* biofilm formation. Future Microbiol. **4:**273–278.
12. **Gaddy JA, Tomaras AP, Actis LA.** 2009. The *Acinetobacter baumannii* 19606 OmpA protein plays a role in biofilm formation on abiotic surfaces and in the interaction of this pathogen with eukaryotic cells. Infect. Immun. **77:**3150–3160.

13. **Loehfelm TW, Luke NR, Campagnari AA.** 2008. Identification and characterization of an *Acinetobacter baumannii* biofilm-associated protein. J. Bacteriol. **190:**1036–1044.
14. **Niu C, Clemmer KM, Bonomo RA, Rather PN.** 2008. Isolation and characterization of an autoinducer synthase from *Acinetobacter baumannii*. J. Bacteriol. **190:**3386–3392.
15. **Tomaras AP, Dorsey CW, Edelmann RE, Actis LA.** 2003. Attachment to and biofilm formation on abiotic surfaces by *Acinetobacter baumannii*: involvement of a novel chaperone-usher pili assembly system. Microbiology **149:**3473–3484.
16. **Brossard KA, Campagnari AA.** 2012. The *Acinetobacter baumannii* biofilm-associated protein plays a role in adherence to human epithelial cells. Infect. Immun. **80:**228–233.
17. **Cucarella C, Solano C, Valle J, Amorena B, Lasa I, Penades JR.** 2001. Bap, a *Staphylococcus aureus* surface protein involved in biofilm formation. J. Bacteriol. **183:**2888–2896.
18. **Eaton TJ, Gasson MJ.** 2002. A variant enterococcal surface protein Esp_{fm} in *Enterococcus faecium*; distribution among food, commensal, medical, and environmental isolates. FEMS Microbiology Lett. **216:**269–275.
19. **Toledo-Arana A, Valle J, Solano C, Arrizubieta MJ, Cucarella C, Lamata M, Amorena B, Leiva J, Penades JR, Lasa I.** 2001. The enterococcal surface protein, Esp, is involved in *Enterococcus faecalis* biofilm formation. Appl. Environ. Microbiol. **67:**4538–4545.
20. **Espinosa-Urgel M, Salido A, Ramos JL.** 2000. Genetic analysis of functions involved in adhesion of *Pseudomonas putida* to seeds. J. Bacteriol. **182:**2363–2369.
21. **Hinsa SM, Espinosa-Urgel M, Ramos JL, O'Toole GA.** 2003. Transition from reversible to irreversible attachment during biofilm formation by *Pseudomonas fluorescens* WCS365 requires an ABC transporter and a large secreted protein. Mol. Microbiol. **49:**905–918.
22. **Latasa C, Solano C, Penades JR, Lasa I.** 2006. Biofilm-associated proteins. C. R. Biol. **329:**849–857.
23. **Wilson K.** 2001. Preparation of genomic DNA from bacteria, p 2.4.1–2.4.5. *In* Ausubel FM (ed), Current protocols in molecular biology. John Wiley & Sons, New York, NY.
24. **Sambrook J, Russell DW.** 2001. Molecular cloning: a laboratory manual, 3rd ed, vol 1. Cold Spring Harbor Laboratory Press, New York, NY.
25. **Sullivan MJ, Petty NK, Beatson SA.** 2011. Easyfig: a genome comparison visualiser. Bioinformatics **27:**1009–1010.
26. **Larkin MA, Blackshields G, Brown NP, Chenna R, McGettigan PA, McWilliam H, Valentin F, Wallace IM, Wilm A, Lopez R, Thompson JD, Gibson TJ, Higgins DG.** 2007. Clustal W and Clustal X version 2.0. Bioinformatics **23:**2947–2948.
27. **Tamura K, Peterson D, Peterson N, Stecher G, Nei M, Kumar S.** 2011. MEGA5: molecular evolutionary genetics analysis using maximum likelihood, evolutionary distance, and maximum parsimony methods. Mol. Biol. Evol. **28:**2731–2739.
28. **Donnelly MI, Zhou M, Millard CS, Clancy S, Stols L, Eschenfeldt WH, Collart FR, Joachimiak A.** 2006. An expression vector tailored for large-scale, high-throughput purification of recombinant proteins. Protein Expr. Purif. **47:**446–454.
29. **Ulett GC, Webb RI, Schembri MA.** 2006. Antigen-43-mediated autoaggregation impairs motility in *Escherichia coli*. Microbiology **152:**2101–2110.
30. **Easton DM, Totsika M, Allsopp LP, Phan MD, Idris A, Wurpel DJ, Sherlock O, Zhang B, Venturini C, Beatson SA, Mahony TJ, Cobbold RN, Schembri MA.** 2011. Characterisation of EhaJ, a new autotransporter protein from enterohemorrhagic and enteropathogenic *Escherichia coli*. Front. Microbiol. **2:**120.
31. **Schembri MA, Klemm P.** 2001. Biofilm formation in a hydrodynamic environment by novel FimH variants and ramifications for virulence. Infect. Immun. **69:**1322–1328.
32. **Kjaergaard K, Schembri MA, Ramos C, Molin S, Klemm P.** 2000. Antigen 43 facilitates formation of multispecies biofilms. Environ. Microbiol. **2:**695–702.
33. **Valle J, Mabbett AN, Ulett GC, Toledo-Arana A, Wecker K, Totsika M, Schembri MA, Ghigo JM, Beloin C.** 2008. UpaG, a new member of the trimeric autotransporter family of adhesins in uropathogenic *Escherichia coli*. J. Bacteriol. **190:**4147–4161.
34. **Heydorn A, Nielsen AT, Hentzer M, Sternberg C, Givskov M, Ersboll BK, Molin S.** 2000. Quantification of biofilm structures by the novel computer program COMSTAT. Microbiology **146:**2395–2407.
35. **Chen CC, Lin YC, Sheng WH, Chen YC, Chang SC, Hsia KC, Liao MH, Li SY.** 2011. Genome sequence of a dominant, multidrug-resistant *Acinetobacter baumannii* strain, TCDC-AB0715. J. Bacteriol. **193:**2361–2362.
36. **Diancourt L, Passet V, Nemec A, Dijkshoorn L, Brisse S.** 2010. The population structure of *Acinetobacter baumannii*: expanding multiresistant clones from an ancestral susceptible genetic pool. PLoS One **5:**e10034. doi:10.1371/journal.pone.0010034.
37. **Imperi F, Antunes LC, Blom J, Villa L, Iacono M, Visca P, Carattoli A.** 2011. The genomics of *Acinetobacter baumannii*: insights into genome plasticity, antimicrobial resistance and pathogenicity. IUBMB Life **63:**1068–1074.
38. **Adams MD, Goglin K, Molyneaux N, Hujer KM, Lavender H, Jamison JJ, MacDonald IJ, Martin KM, Russo T, Campagnari AA, Hujer AM, Bonomo RA, Gill SR.** 2008. Comparative genome sequence analysis of multidrug-resistant *Acinetobacter baumannii*. J. Bacteriol. **190:**8053–8064.
39. **Park SJ, Chao G, Gunsalus RP.** 1997. Aerobic regulation of the *sucABCD* genes of *Escherichia coli*, which encode α-ketoglutarate dehydrogenase and succinyl coenzyme A synthetase: roles of ArcA, Fnr, and the upstream *sdhCDAB* promoter. J. Bacteriol. **179:**4138–4142.
40. **Pierard A, Glansdorff N, Gigot D, Crabeel M, Halleux P, Thiry L.** 1976. Repression of *Escherichia coli* carbamoylphosphate synthase: relationships with enzyme synthesis in the arginine and pyrimidine pathways. J. Bacteriol. **127:**291–301.
41. **Li K, Jiang T, Yu B, Wang L, Gao C, Ma C, Xu P, Ma Y.** 2012. Transcription elongation factor GreA has functional chaperone activity. PLoS One **7:**e47521. doi:10.1371/journal.pone.0047521.
42. **Cucarella C, Tormo MA, Ubeda C, Trotonda MP, Monzon M, Peris C, Amorena B, Lasa I, Penades JR.** 2004. Role of biofilm-associated protein *bap* in the pathogenesis of bovine *Staphylococcus aureus*. Infect. Immun. **72:**2177–2185.
43. **Deng W, Liou SR, Plunkett G, Mayhew GF, Rose DJ, Burland V, Kodoyianni V, Schwartz DC, Blattner FR.** 2003. Comparative genomics of *Salmonella enterica* serovar typhi strains Ty2 and CT18. J. Bacteriol. **185:**2330–2337.
44. **Huber B, Riedel K, Kothe M, Givskov M, Molin S, Eberl L.** 2002. Genetic analysis of functions involved in the late stages of biofilm development in *Burkholderia cepacia* H111. Mol. Microbiol. **46:**411–426.
45. **Jordan SJ, Perni S, Glenn S, Fernandes I, Barbosa M, Sol M, Tenreiro RP, Chambel L, Barata B, Zilhao I, Aldsworth TG, Adriao A, Faleiro ML, Shama G, Andrew PW.** 2008. *Listeria monocytogenes* biofilm-associated protein (BapL) may contribute to surface attachment of *L. monocytogenes* but is absent from many field isolates. Appl. Environ. Microbiol. **74:**5451–5456.
46. **Latasa C, Roux A, Toledo-Arana A, Ghigo JM, Gamazo C, Penades JR, Lasa I.** 2005. BapA, a large secreted protein required for biofilm formation and host colonisation of *Salmonella enterica* serovar Enteritidis. Mol. Microbiol. **58:**1322–1339.
47. **Roux A, Beloin C, Ghigo JM.** 2005. Combined inactivation and expression strategy to study gene function under physiological conditions: application to identification of new *Escherichia coli* adhesins. J. Bacteriol. **187:**1001–1013.
48. **Stalhammar-Carlemalm M, Areschoug T, Larsson C, Lindahl G.** 1999. The R28 protein of *Streptococcus pyogenes* is related to several group B streptococcal surface proteins, confers protective immunity and promotes binding to human epithelial cells. Mol. Microbiol. **33:**208–219.
49. **Stockbauer KE, Fuchslocher B, Miller JF, Cotter PA.** 2001. Identification and characterisation of BipA, a *Bordetella* Bvg-intermediate phase protein. Mol. Microbiol. **39:**65–78.
50. **Tormo MA, Knecht E, Gotz F, Lasa M, Penades JR.** 2005. Bap-dependent biofilm formation by pathogenic species of *Staphylococcus*: evidence of horizontal gene transfer? Microbiology **151:**2465–2475.
51. **Walter J, Chagnaud P, Tannock GW, Loach DM, Dal Bello F, Jenkinson HF, Hammes WP, Hertel C.** 2005. A high-molecular-mass surface protein (Lsp) and methionine sulfoxide reductase B (MsrB) contribute to the ecological performance of *Lactobacillus reuteri* in the murine gut. Appl. Environ. Microbiol. **71:**979–986.
52. **Newell PD, Boyd CD, Sondermann H, O'Toole GA.** 2011. A c-di-GMP effector system controls cell adhesion by inside-out signaling and surface protein cleavage. PLoS Biol. **9:**e1000587. doi:10.1371/journal.pbio.1000587.
53. **Rahbar MR, Rasooli I, Gargari SLM, Amani J, Fattahian Y.** 2010. In silico analysis of antibody triggering biofilm associated protein in *Acinetobacter baumannii*. J. Theor. Biol. **266:**275–290.